2015

Tail-Assisted Rigid and Compliant Legged Leaping

Anna Brill
anbrill@seas.upenn.edu

Avik De
avik@seas.upenn.edu

Aaron Johnson
amj1@cmu.edu

Daniel Koditschek
kod@seas.upenn.edu

Tail-Assisted Rigid and Compliant Legged Leaping

Abstract
This paper explores the design space of simple legged robots capable of leaping culminating in new behaviors for the Penn Jerboa, an underactuated, dynamically dexterous robot. Using a combination of formal reasoning and physical intuition, we analyze and test successively more capable leaping behaviors through successively more complicated body mechanics. The final version of this machine studied here bounds up a ledge 1.5 times its hip height and crosses a gap 2 times its body length, exceeding in this last regard the mark set by the far more mature RHex hexapod. Theoretical contributions include a non-existence proof of a useful class of leaps for a stripped-down initial version of the new machine, setting in motion the sequence of improvements leading to the final resulting performance. Conceptual contributions include a growing understanding of the Ground Reaction Complex as an effective abstraction for classifying and generating transitional contact behaviors in robotics.

Disciplines
Electrical and Computer Engineering | Engineering | Systems Engineering

Tail-Assisted Rigid and Compliant Legged Leaping

Anna L. Brill* Avik De* Aaron M. Johnson† Daniel E. Koditschek*

***Abstract*— This paper explores the design space of simple legged robots capable of leaping culminating in new behaviors for the Penn Jerboa, an underactuated, dynamically dexterous robot. Using a combination of formal reasoning and physical intuition, we analyze and test successively more capable leaping behaviors through successively more complicated body mechanics. The final version of this machine studied here bounds up a ledge 1.5 times its hip height and crosses a gap 2 times its body length, exceeding in this last regard the mark set by the far more mature RHex hexapod. Theoretical contributions include a non-existence proof of a useful class of leaps for a stripped-down initial version of the new machine, setting in motion the sequence of improvements leading to the final resulting performance. Conceptual contributions include a growing understanding of the Ground Reaction Complex as an effective abstraction for classifying and generating transitional contact behaviors in robotics.**

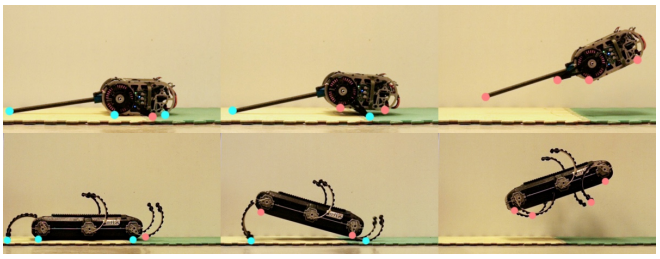

Fig. 1. Similar leaps executed on Jerboa [2] (**top**) and RHex [4] (**bottom**, from [1]) showing similar qualitative behavior in response to similar control policies despite significant kinematic and dynamic differences (Table I). These transitional behaviors are difficult to analyze with classical dynamical systems theory since they cannot be encoded in terms of stable attractors and their dynamics change depending on which subset of ground contacts is active (**cyan**) or inactive (**magenta**).

I. Introduction

This paper develops a novel combination of intuition and formal reasoning originated in [1] to generate a variety of leaps on the Penn Jerboa [2] (an tailed biped whose four actuators are dynamically coupled across twelve degrees of freedom) with the aim of exciting a diverse array of energetic behaviors. The machine bounds up a ledge one and one half its hip height and crosses a gap of nearly two bodylengths—the former achieving and the latter exceeding the mark set by [1]. Such highly energetic, agile transitional maneuvers uniquely distinguish the province of legged mobility [3] from its wheeled and tracked counterparts.

While the details of leaping height and distance reported here do not result from any explicit optimization, we observe and carefully report on their structural sensitivity to platform and controller design (e.g., see Fig. 7). This phenomenon is relatively unexplored in the prior literature and speaks to a need for new theoretical approaches to this class of non-steady behaviors. The growing strength of the methods we use to reason about and achieve them likely represents the most enduring value of this work.

Specifically, our main contributions toward the goal of understanding and achieving repeatable non-steady leaping across diverse legged platforms include: (a) drawing from a new hybrid systems self-manipulation model [5] empirically-validated analytical insights concerning the interaction of mechanical design with behavioral dexterity (Section II); (b) marshaling empirical evidence to suggest the efficacy of the Ground Reaction Complex (GRC) abstraction [1]—not merely for exhaustively navigating the space of possible leaps, but for revealing the similar consequences of similar leaps executed by two radically dissimilar and seemingly incomparable morphologies (Section III); and (c) empirical demonstration of novel behaviors with useful real world applications (Section IV).[1] We now describe each of these results in detail.

In Section II we consider a "tailless" version of the Jerboa, arguably the simplest general purpose mechanism with which one could imagine oriented leaps. The first use of its simple 3-contact GRC, [1], Section II-A, is to achieve result (a), summarized above. Namely, the GRC organizes our analytical investigation of the "tailless" machine's (relatively) simple associated self-manipulation hybrid system [5, 6] dynamics, Section II-B, leading up to the key formal conclusion of the paper (Prop. 1): a centered hip, rigid leg version of the mechanism cannot achieve a level leap with any control policy (Section II-C). To avoid this problem, Sections II-D introduces a novel way to use compliance in the legs [7], and hybrid self-manipulation [5] simulations of a compliant tailless Jerboa in Section II-E indicate this more complicated machine can achieve level leaps that outperform a rigid leg—and further outperforms even a dedicated (prismatic shank-energized) vertical hopper (Fig. 3). Section II-F presents physical experiments with the compliant limb (Table II).

Although improved, the empirical leaping performance

*Electrical and Systems Engineering, University of Pennsylvania, Philadelphia, PA, USA. {anbrill,avik,kod}@seas.upenn.edu.

†Robotics Institute, Carnegie Mellon University, Pittsburgh, PA, USA.

This work was supported in part by the ARL/GDRS RCTA project, Coop. Agreement #W911NF-10-2-0016 and in part by NSF grant #1028237.

[1]Note that we are concerned in this paper with behaviors ("leaps") rather than the specific control strategies to achieve them. Accordingly, we rely here upon open loop strategies since these suffice to elicit the behaviors of interest. An important question lying beyond the scope of this paper concerns the development of a "reference signal" appropriate to these combinatorially intricate hybrid dynamical systems flows relative to which a closed loop control formalism might be introduced.

(e.g., in gap crossing and ledge height comparisons) of the compliant tailless version of the Jerboa is still not competitive with that of the XRL variant of RHex [4]. In Section III we take the step of giving the Jerboa back the use of its tail to provide a 4-contact system suitable for direct comparison with RHex [1]. Traditionally in robotics, a tail is thought of as an inertial appendage, whose reaction forces can be used to rapidly reorient the body [8–10], provide power [11, 12], or stabilize its locomotion [13, 14]. There have also been some examples of robots using a passive tail to interact with the environment as an additional support [15, 16]. However, there is biological precedent for dynamic tails acting through ground interaction [17], and we believe this paper presents the first robotic example of a tail used solely in this way.

The hybrid self-manipulation model [5] of the tailed Jerboa is complicated enough that a formal inquiry (such as presented in Section II for the three-contact GRC) far exceeds our present scope. We are, however, able to check numerically whether these physically simplified, mathematically tractable models are sufficiently accurate to lend believable design insight. Specifically, we compare the physical tailed Jerboa with a simulation of our self-manipulation hybrid model and find a close correspondence (Fig. 5). We observe, in Section III-A, that the tailed Jerboa's GRC is identical in structure to that of RHex as deployed in [1], yielding result (b), summarized above. First, we proceed to use the GRC as a guide to organize the design of controllers to empirically exercise the new machine's more complicated behaviors. Second, Fig. 1 suggests (and Section III-B, Fig. 7 documents) the two machines' behavioral correspondence (respecting what we term "word boundary discontinuity") in response to similar inputs notwithstanding their different kinematics and dynamics (Table I). Moreover, the Jerboa's performance now approaches that of RHex (Table II, columns 2 and 4).

As to the source of the improved performance, Table I suggests that while RHex's greater force density may give it an edge in the single leaping tasks that represent the formal focus of this paper, Jerboa's greater power density and specific agility [18] ought to lend some advantage in tasks involving the harvesting and transduction of energy. Thus, in Section IV we discuss how a more intuitive use of the formal and informal reasoning originating in [1] leads to a successful round of double jumps on Jerboa (Table II, columns 3 and 5) that allow it to match or exceed the performance of RHex, and we suggest how such leaps are potentially applicable in complete behaviors, comprising result (c), summarized above. The paper concludes in Section V with some brief speculative remarks concerning future designs and analysis.

II. Leaping with a Revolute Leg

Our first model system of interest is a planar rigid body, $x, z, \phi \in \mathrm{SE}(2)$, with only a 1DOF massless[2] revolute leg, moving through a hip angle $\theta_1 \in S^1$ (leg-body angle), as shown in Fig. 2. Even though it seems unconventional to perform leaping tasks (nominally, lifting the center of mass vertically) without any direct "leg extension" affordance, this morphology has (a) been used in the past with demonstrably energetic leaps on RHex [1], and (b) provides arguably the simplest instance of a body with sufficient degrees of freedom (to offer a usefully rich set of apex states), but at the same time a sufficiently low-dimensional control space (such that it is feasible to search in order to discover the expanse of possible behaviors).

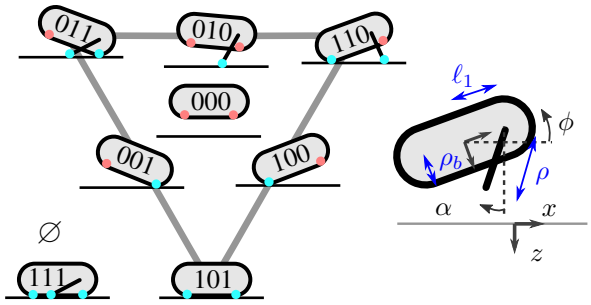

Fig. 2. The monopedal model of Section II has three possible contact points: the nose, the leg, and the rear. The GRC for this model is shown on the **left**, generated from the two body (sliding) rolling contacts, and a (sticking—Assumption 2) point toe. The $\varnothing$-simplex is the fully constrained mode, 111, is shown in the corner and has trivial, degenerate dynamics, but generically the robot must pass through it for each leap. The cartoons drawn in the complex have pink (cyan) dots for inactive (active) contacts, respectively. On the **right**, we show the system parameters (blue), and the configuration variables (black). The analysis of Section II-C assumes $\ell_1 = 0$ for analytical tractability (Assumption 1, but we relax this assumption in our numerical (Section II-E) and empirical (Section II-F) tests.

In fact, we show simulations results in Section II-E that suggest an equivalent shank-actuated system can be matched or surpassed in performance by this revolute-actuated system.

A. The 3-contact GRC

The *Ground Reaction Complex* (GRC) [1] is a combinatorial structure summarizing the dimension and adjacency relations of a limbed robot's contacts with its environment [1]. Intuitively, the GRC (e.g. in Fig. 2) encodes the contact modes and how they relate to each other, capturing all of the discrete structure of the model. We use the GRC to reason about different behaviors by enumerating all of the logically possible paths through this cell complex, and then quickly restricting down to only the feasible leaping paths.

Namely, the GRC is an abstract simplicial complex (see e.g.. [20, Sec. III.1]) whose cells represent *contact modes* [5], i.e., collections of active contact constraints. For the purposes of this paper, the vertices correspond to modes that are characterized by all but one active contact constraint, the edges are characterized by all but two constraints, and so on. The null set (an element of any simplicial complex) is the fully constrained mode.[3]

As shown in Fig. 2, the set of possible contacts with the ground for the monopedal model is {N, L, R}, (corresponding to the Nose, Leg, and Rear) and the contact modes will

[2]The combined mass of the legs (and later tail) of the Jerboa is $< 10\%$ of the body mass (Table I), and we find it justifiable [6] to ignore the effects of limb inertia on attitude.

[3]This definition implies that, for the example in Fig. 2, each cell in the complex will have one fewer dimension than the kinematic freedoms of its corresponding contact mode.

be denoted as a string of binary bits such as 110 or 000 (representing the contact modes {N, L} or {}, respectively). This allows for 8 possible contact modes or "letters", appearing as cells (edges, vertices, etc) of the complex. Adjacency relationships (faces and cofaces) represent logically possible transitions[4]. The highest-dimension cell (000, no contact) is the desired "final" simplex for the leaping task, and the bottom vertex (101, body on the ground) is the "initial" cell.

Following the logic of [1, Sec. III.C], of all possible paths (or "words", i.e. sequences of letters) in the GRC from 101 to 000, we find that only two are dynamically viable and acyclic, i.e. those that agree with the continuous dynamics (in the sense of [5], unlike, e.g., 101 → 100), results in a leaping behavior (as will be defined in Defn. 1), and where each contact touches down or lifts off at most once:

Leap 1: 101 → 111 → 011 → 010 → 000
Leap 2: 101 → 111 → 110 → 010 → 000

As a result of Assumption 1, $\ell_1 = 0$, there is a mirror symmetry between letters 011 & 110 and, consequently, we limit our analysis to Leap 1 as the two leaps are equivalent. With this three contact GRC now defined and reduced to a single word of interest, we now explore the continuous dynamics of this word.

B. Self-manipulation Modeling

In this section we derive the kinematics, dynamics, and transition conditions necessary for the proof of Prop. 1 for Leap 1, focusing on contact mode 010 but also including some aspects of 000 and 011. We express these equations of motion by following [5, 6], which we summarize here.

Recall that in this rigid-leg model the configuration space is, $\mathbf{q} := (\theta_1, x, z, \phi)$. Define also the absolute leg angle,

$$\alpha := \theta_1 - \phi, \text{ and } v := \begin{bmatrix} -\sin\alpha \\ \cos\alpha \end{bmatrix}, \tag{1}$$

where v is a unit vector aligned with the leg.

Each contact mode K (i.e. each set of active contact constraints) is subject to a base constraint, $\mathbf{a}_K(\mathbf{q}) = 0$, [6, Eqn. 9], and a derived velocity constraint, $\mathbf{A}_K(\mathbf{q})\dot{\mathbf{q}} = 0$. The inertia tensor, [6, Eqn. 26], is,

$$\mathbf{M} = \begin{bmatrix} 0 & \\ & \mathbf{M}_b \end{bmatrix}, \text{ where } \mathbf{M}_b := \begin{bmatrix} m_b I & \\ & i_b \end{bmatrix}, \tag{2}$$

however, following [5, 6], when the leg is unconstrained (in the air) we may drop it from the dynamics and use simply $\mathbf{M}_b$ as the inertia tensor. The potential energy and actuator forces, [6, Eqns. 27, 31], are the same in all modes,

$$V(\mathbf{q}) := -m_b g z, \qquad \Upsilon := \begin{bmatrix} \tau_1 \\ 0 \end{bmatrix}. \tag{3}$$

The full dynamics in mode K, [6, Eqn. 33], are,

$$\begin{bmatrix} \mathbf{M} & \mathbf{A}_K^T \\ \mathbf{A}_K & 0 \end{bmatrix} \begin{bmatrix} \ddot{\mathbf{q}} \\ \lambda \end{bmatrix} = \begin{bmatrix} \Upsilon - \mathbf{N} \\ -\dot{\mathbf{A}}_K \dot{\mathbf{q}} \end{bmatrix}, \tag{4}$$

where λ are the constraint forces (e.g in mode 010, $\lambda = \begin{bmatrix} \lambda_t \\ \lambda_n \end{bmatrix}$, normal and tangential toe forces), and $\mathbf{N}$ is the force due to the potential energy, $V(\mathbf{q})$, [6, Eqn. 31]. Note that here there are no Coriolis or centrifugal forces, [6, Eqn. 30]. Observe that the left-hand matrix in (4) is invertible, even though $\mathbf{M}$ is not, [5, Eqn. 9]. Continuing to follow [5, 6] the equations of motion obtained by rearranging (4) are,

$$\begin{bmatrix} \ddot{\mathbf{q}} \\ \lambda \end{bmatrix} = \begin{bmatrix} \mathbf{M}_K^\dagger \mathbf{A}_K^{\dagger T} \\ \mathbf{A}_K^\dagger \ \mathbf{\Lambda}_K \end{bmatrix} \begin{bmatrix} \Upsilon - \mathbf{N} \\ -\dot{\mathbf{A}}_K \dot{\mathbf{q}} \end{bmatrix}, \tag{5}$$

Up to II-C, we make the following assumption for analytical tractability:

Assumption 1 (Design assumptions)**.** *The center of mass is coincident with the hip ($\ell_1 = 0$), and the leg is long enough to clear the body, $\rho_b + \ell_b < \rho$.*

Nonetheless, we present simulation (Section II-E) as well as empirical (Section II-F) results without this assumption and find that Prop. 1 is still relevant. We also make the following assumption about the friction cone constraints:

Assumption 2 (Sticking toes)**.** *The toe never slides.*

1) Mode 000: In analyzing Leap 1, first consider the final "letter," mode 000. As there are no contact constraints or reaction forces, the equations of motion are quite simple—the only force is gravity and so,

$$\ddot{z}|_{000} = g, \qquad \ddot{x}|_{000} = \ddot{\phi}|_{000} = 0. \tag{6}$$

2) Mode 010: Working backwards from the final apex condition, we next consider the penultimate letter, contact mode 010. From (5), the pitch dynamics are

$$\ddot{\phi} = \tau_1 / i_b. \tag{7}$$

Finally, consider the liftoff conditions for this contact mode. As a consequence of Assumption 2, liftoff can only happen when $\lambda_n = 0$. From the second block-row of (5),

$$\lambda_n = \tfrac{\tau_1 \sin\alpha}{\rho} + (m_b \rho \dot{\alpha}^2 - m_b g \cos\alpha)\cos\alpha. \tag{8}$$

3) Mode 011: Continuing to progress backwards through Leap 1, from mode 011, corresponding to the leg and rear body contacting the ground, we will only need one element of the velocity constraint,

$$-\dot{z} + \rho_b \cos\phi \dot{\phi} = 0 \implies \dot{\phi} = \tfrac{\dot{z}}{\rho_b \cos\phi}, \tag{9}$$

and the kinematic bounds,

$$-\pi/2 < \phi|_{011} \leqslant 0 \implies \cos(\phi|_{011}) > 0, \tag{10}$$

and therefore $\dot{\phi}|_{011}$ will have the same sign as $\dot{z}$. The kinematic base constraint includes,

$$-z - \rho_b + \ell_b \sin\phi = 0, \quad -z - \rho\cos\alpha = 0, \tag{11}$$

which (together with Assumption 1) can be used to get bounds on α,

$$0 \leqslant \tfrac{\rho_b}{\rho} \leqslant \cos(\alpha|_{011}) \leqslant \tfrac{\rho_b + \ell_b}{\rho} < 1, \tag{12}$$

which implies that α cannot change sign within 011, as $\alpha|_{011} \neq 0$.

[4]The physically available hybrid system transitions are a subset of the star of the closure of a given cell in the GRC as determined by the complementarity conditions, [5].

4) Modes 111 and 101: From mode 101 the massless leg will touch down and the system will enter 111 with no impulse (as there was no momentum). However in mode 111 with any applied torque pushing the leg into the ground the nose body contact force is such that it will immediately detach according to the force–acceleration complementarity conditions [5, Eqn. 37], again with no impulse or discontinuity in state[5]. Therefore we omit any further discussion of these contact modes.

C. Level Leaps

In this section, we develop necessary conditions for a "level" leap, by which we mean that the pitch at apex, $\phi_{\text{apex}} = 0$. Define the cell entry time, t_K, as the time that the execution enters contact K (i.e. t_{000} is the time the execution entered contact mode 000, the aerial mode).

Definition 1 (Leaping behavior)**.** *We restrict to a class of leaping behaviors where (a) the body is ascending ($\dot{z} < 0$) until apex is reached, and (b) $z(t_{000}) - z_{\text{apex}} \geqslant \rho/2$.*

Without loss of generality, we consider here only Leap 1, where the leg is starting on the and rotating counterclockwise, i.e. $\theta_1(t_{111}) > 0$, $\phi(t_{111}) = 0$, and so $\alpha(t_{111}) > 0$.

We are now ready to state the central result of this section:

Proposition 1. *With the rigid-leg body of Fig. 2 and assumption 1, it is impossible to get a level leap.*

The following Lemmas help organize the proof:

Lemma 1. *Torque reversal (sign change in τ_1 [1, IV-B]) in mode 010 is* necessary *for a level leaping behavior.*

Proof. The transition from 011 to 010 at time t_{010} is a liftoff event where we only remove a constraint, and so there is no *contact impulse* [5]. As the position and velocity (in particular the ϕ and $\dot{\phi}$ components) are continuous at time t_{010}, (9)–(10) also describe the pitch after the transition to mode 010. Thus $\phi(t_{010}) < 0$ and $\dot{\phi}(t_{010}) < 0$ (as $\dot{z} < 0$, Defn. 1, and therefore $\dot{\phi}(t)|_{011} < 0$).

Therefore a necessary condition for level pitch ($\phi = 0$), is that at some point the pitch acceleration be greater than zero. Furthermore the transition to the aerial state, $010 \to 000$, is also a liftoff transition (with ϕ, $\dot{\phi}$ continuous), and the pitch acceleration is zero in the aerial state, (6). Therefore the positive pitch acceleration must occur in the 010 mode, i.e. $\exists t, t_{010} < t < t_{000}, \ddot{\phi}(t) > 0$. From (7), we see that the hip torque, τ_1, is the only mechanism available for pitch correction in this contact mode. We conclude that it is necessary to have $\tau_1 > 0$ for some time in mode 010. □

Lemma 2. *Torque reversal in letter 010 is* sufficient *for inducing liftoff from $010 \to 000$ at t_s.*

Proof. Recall that initially $\alpha(t_{111}) > 0$. The transition to mode 011 is instantaneous and, like all transitions continuous in the base, i.e. $\alpha(t_{011}) > 0$. Kinematically in mode 011 α cannot change sign, (12), and so $\alpha(t_{010}) > 0$. From the closed-loop constraint pinning the toe in mode 010,

$$\dot{x} = \rho \cos\alpha\dot{\alpha}, \qquad \dot{z} = \rho \sin\alpha\dot{\alpha}, \tag{13}$$

and Defn. 1 we see that $\alpha\dot{\alpha}|_{010} < 0$ (as $\dot{\alpha}(t)$ is a continuous function of time, $\dot{z} = \rho \sin\alpha\dot{\alpha}$ is positive the instant after α crosses 0 from above). Consequently α cannot cross 0 in letter 010, $\alpha|_{010} > 0$, and furthermore $\dot{\alpha}|_{010} < 0$.

From (5), we get,

$$\ddot{\alpha} = \ddot{\theta}_1 - \ddot{\phi} = \tfrac{\tau_1}{m_b\rho^2} + \tfrac{g\sin\alpha}{\rho}. \tag{14}$$

Consider the effect of torque reversal, i.e. define t_s as the minimal time that the torque is positive, $\tau(t_s) \geqslant 0$ and $\forall t < t_s, \tau(t) < 0$. Thus at the time of torque reversal (if not sooner), $\ddot{\alpha}(t) > 0$ and therefore,

$$\tfrac{d}{dt}\dot{\alpha}^2(t_s) = 2\dot{\alpha}(t_s)\ddot{\alpha}(t_s) < 0 \tag{15}$$

After the transition to 000, integrating the flight dynamics, (6), we see that $z(t_{000}) - z_{\text{apex}} = \dot{z}^2(t_{000})/2g$. The energetic assertion made about the behavior (Defn. 1) implies liftoff condition for the minimum desired velocity to be a viable leap,

$$\dot{z}^2(t_{000}) = 2g(z(t_{000}) - z_{\text{apex}}) \geqslant g\rho. \tag{16}$$

Using the closed loop constraint in mode 010 just before takeoff, (13), we can convert this liftoff condition on $\dot{z}(t_{000})$ to a condition on $\dot{\alpha}(t_{000})$,

$$\rho\dot{\alpha}(t_{000})^2 \geqslant \tfrac{g}{\sin^2\alpha(t_{000})} \implies \rho\dot{\alpha}(t_{000})^2 - g \geqslant 0, \tag{17}$$

Therefore there are two possibilities: either (i) the minimum liftoff condition, (17), is already met at t_s and the liftoff could be viable, or (ii) the minimum liftoff condition has not been met yet at t_s and the liftoff cannot be viable (as $\dot{\alpha}^2$ will continue to decrease, (15), but not reach zero as $\dot{\alpha} < 0$). As only case (i) leads to a leap that meets the requirements of Defn. 1, we can assume $\rho\dot{\alpha}(t_s)^2 - g \geqslant 0$, and further observing that $0 \leqslant \cos\alpha \leqslant 1$, we get the bound,

$$\rho\dot{\alpha}(t_s)^2 - g\cos\alpha(t_s) \geqslant 0. \tag{18}$$

Applying to the liftoff condition (8),

$$\begin{aligned}\lambda_n(t_s) &= \tfrac{\tau_1 \sin\alpha(t_s)}{\rho} + m_b\cos\alpha(t_s)(\rho\dot{\alpha}(t_s)^2 - g\cos\alpha(t_s)) \\ &\geqslant \tfrac{\tau_1\sin\alpha(t_s)}{\rho}.\end{aligned}$$

Hence $\tau_1 \geqslant 0$ is a sufficient condition for λ_n crossing zero from below and liftoff occurring. □

Proof of Prop. 1. Through Lemmas 1 and 2, we have shown that for leap word 1, (a) pitch correction is only possible through torque reversal, and (b) torque reversal causes immediate liftoff. Lastly, we note that even though performed the analysis above for leap word 1, the result holds similarly for leap word 2 by symmetry induced by Assumption 1. □

[5]If the leg mass were small but not zero, the hybrid execution will skip over mode 111 since the impulse–velocity complementarity condition would not be satisfied at any leg velocity [5, Lemma 10]. In the formalism of this paper mode 111 is still included as a logical adjacency.

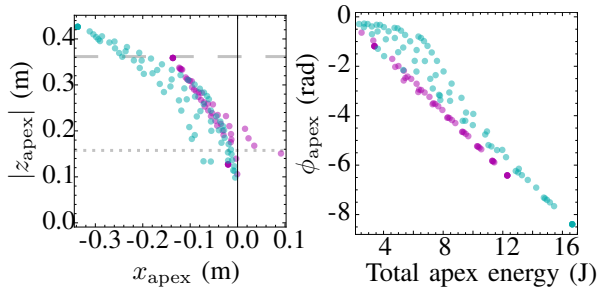

Fig. 3. Simulation apex states obtained from leap 1 (II-E), with a rigid (pink) and compliant (cyan) leg, when sweeping over the two control parameters of (21). The compliant leg has a point contact and Hooke's law spring constant 3000 N/m. The dotted horizontal line is the minimum apex height stipulated in Defn. 1, and the dashed line corresponds the apex height reached by an equivalent 1DOF shank-actuated leaper[7].

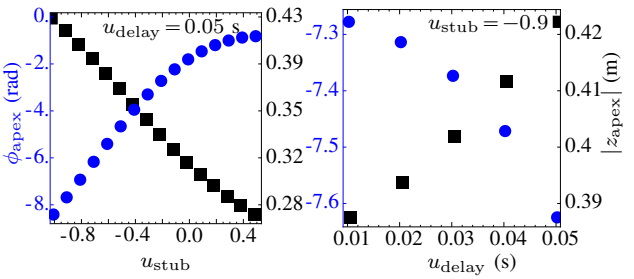

Fig. 4. Simulation results of pitch correction by "stubbing" (Sec. II-B), showing that varying u_{stub} trades off between apex pitch and apex height. The delay parameter, u_{delay} has a much smaller effect on apex state.

D. Introduction of Compliance

The result above suggests that some additional leg DOF is required to get level leaps, either through an increase in the control affordance or in the underlying dynamics of the Jerboa. We choose the latter option to explore here and introduce a series-elastic compliant element to the leg. We omit a complete analysis of this new 5DOF system, but point out the following consequences of adding leg compliance which we conjecture are paramount to the qualitatively better leaps observed both numerically (Section II-E) and empirically (Section II-F):

i) The liftoff equation (8) changes to

$$\lambda_n = \mathrm{D}\varphi \cos\alpha + \tfrac{\tau_1 \sin\alpha}{\ell}, \tag{19}$$

where ℓ is the leg length (replacing the constant length ρ), and the spring potential is denoted by $\varphi(\mathbf{q})$. The loaded spring provides added normal force $\mathrm{D}\varphi$, providing more freedom in τ_1 without inducing liftoff.

ii) Lemma 1 still holds, but Lemma 2 is not true any more, and reversal torques can be used to do pitch correction.

iii) The kinematic constraint in 010 relating $\dot{z}$ to $\dot{\alpha}$ is now

$$\dot{z} = \cos\alpha\,\dot{\ell} - \ell \sin\alpha\,\dot{\alpha}, \tag{20}$$

somewhat decoupling $\dot{z}$ from α. In fact, from our empirical testing (Section II-F), the leg extends as the spring unloads before liftoff, allowing $\dot{z} < 0$ even when the leg is vertical ($\alpha = 0$).

E. Numerical Results

We use a simulation environment in Mathematica (a computational implementation of the hybrid systems formulation of [5]) to sweep the following parameterization of the control space (motivated by [21], [1, IV-B] and Prop. 1):

Definition 2 ("Stubbing" control strategy)**.** *We restrict to a 2-parameter family of controllers where the applied torque is a function of the parameters*[6] $(u_{\text{stub}}, u_{\text{delay}})$*,*

$$\tau_1 = \begin{cases} -\tau_{\max} & \text{if } t < t_{010} + u_{\text{delay}} \\ u_{\text{stub}}\tau_{\max} & \text{if } t_{010} + u_{\text{delay}} < t, \end{cases} \tag{21}$$

In implementation (Fig. 3), $u_{\text{delay}} \in [0.01, 0.05]$ s and $u_{\text{stub}} \in [-1, 0.5]$. Intuitively, u_{delay} must be small enough that the stubbing has time to act before liftoff (transition to 000), and u_{stub} must be small enough that the apex state is of sufficient (Defn. 1) energy. Note that (i) this is a revision of the relative-timing controller [1] which produced a rich array of energetic leaps on RHex, necessitated by the presence of only a single appendage, and (ii) "stubbing" is an instance of torque reversal (Prop. 1), where we parameterize the switching time and magnitude, but a relaxation in that we allow for reduction of torque ($|\tau_1| < |\tau_{\max}|$) without a sign change as well.

The system parameters are chosen to closely match our physical platform (Fig. 2, Table I), relaxing Assumption 1 to achieve greater physical fidelity (at the expense of greater analytical complexity) in the process. Lastly, we add a motor model [22], so that the control affordance over θ_1 in (21) is over voltage and not directly over torque.

In Fig. 3, we have plotted the apex states corresponding to a sweep over our control input parameter space (21). We present apex (x, z) positions on the left plot, and on the right, we plot "almost level" leaps, corresponding to $|\phi_{\text{apex}}| < \pi/4$. Observe that

i) we get a greater number of almost-level leaps, and in general a larger volume of possible apex states, with a compliant leg,

ii) the compliant leaps yield a greater total kinetic energy (the greater apex height is clearly visible in the figure)

Fig. 3 also shows (as a dashed horizontal line) the apex height attained by an equivalent[7] 1DOF shank-actuated robot, showing that the hip-actuated system has comparable performance to the morphologically specific 1DOF leaper.

[6]Specifically, $-1 < u_{\text{stub}} < 1$, with positive values indicating "reversal." The parameter u_{delay} is designed to avoid flow-discontinuities near the guard set, which could possibly result in a Zeno-like event [5].

[7]We assume the shank-motor robot has mass identical to the revolute-hip robot, it is powered by an actuator which has a stroke length budget assumed to be $\rho - \rho_b$, the same power as the hip motor of the system in Fig. 2, and a gearbox is optimally chosen for the leaping task [22].

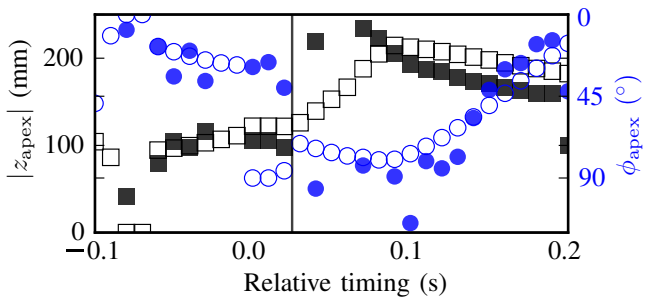

Fig. 5. Height (black square) and pitch (blue circle) apex data from the Jerboa (filled) and simulation (hollow), across a range of the relative timing parameter [1], showing reasonable agreement between empirical trials and our simulation environment built upon the hybrid systems framework of [5]. There were larger discrepancies in the horizontal displacement data points (not shown), at least in part attributable to our modeling of the body and tail as idealized sliding contacts—which is difficult to match in practice.

In Fig. 4, we plot the sensitivity of the apex state to the reversal parameter, u_{stub} and delay parameter u_{delay}, showing that the reversal strategy has significant utility for planning control sequences to attain desired apex states.

F. Empirical Results

We use the Jerboa (Table I) with its tail removed as the physical testbed for this section. As predicted by theory and simulation, a rigid-legged robot either fails to get airborne with sufficient energy (high u_{stub}), or spins rapidly through the air (attached video). The introduction of a half-circle compliant leg (with its additional complexity and benefits detailed in IV) results in controllable apex pitch. Qualitatively, the leaps found in this way are suitable for a gap-crossing of 0.27 m or 1.29 body lengths, and a ledge ascent of 9 cm or 0.9 hip heights, using a single actuator.

III. Leaping with a Leg and a Tail

In this section we address the limitations of the 3-contact model, including the provable behavioral incapability (Proposition 1) in its rigid form, by adding another actuated degree of freedom—the Jerboa with active tail (see Fig. 1). The tail length is approximately two leg lengths, has negligible inertia compared to the rest of the robot, and (in this paper) is chosen to act only through physical ground interaction.

In so doing, we establish an exact correspondence with the very different (see Table I) RHex platform explored in [1] via their common 4-contact GRC (graphically a simplicial tetrahedron pictured in [1, Fig. 3a], omitted here for space). In advance of more practical questions concerning the relative utility of the resulting Jerboa leaps (to be taken up in Section IV), the focus of this section will instead be on this common structure and how qualitatively alike the physically realizable 4-contact leaps of these different robots are.

The 4-contact version of the Jerboa consists of a planar 3-DOF rigid body, a revolute, massless leg and a tail—a second longer appendage not designed to support the weight of the body, but that can still interact with the world. The contact set is similar to Section II-A but with the inclusion of a fourth contact point, {N, L, R, T}, and is the same

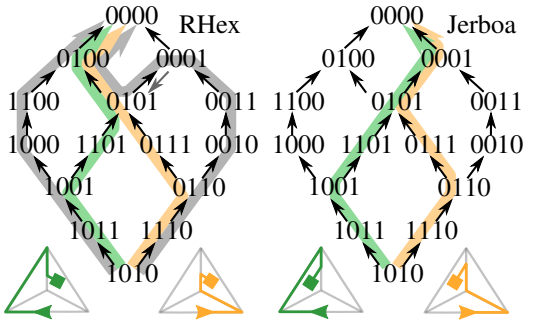

Fig. 6. Leap words realized on the Jerboa, juxtaposed with those realized on RHex [1] using a range of $(+,-)$ relative leg timing[8]. The main RHex leaps are a front/rear reflection of the Jerboa leaps. (See Section III)

as [1] up to naming. Finally, while [1] focused on leaps with all legs pushing "forward", $(+,+)$, the kinematics of the Jerboa model do not allow the tail to be used in the forward configuration, and so we will compare with the $(+,-)$ leap, where one set of legs push forward and the other pushes backwards [1, Fig. 5]. In order to keep our controller parameterization low-dimensional for systematic trials, we adopt the single timing parameter of [1], and exercise the stubbing controller-DOF in a more exploratory way in Section IV.

A. Leap Words

While the modes of any 4-contact GRC are related by combinatorially intrinsic adjacencies and hence determine a fixed graph of logically possible pairwise transitions, different kinematics and mechanics will result in different physically realizable transitions. This pruned directed graph of the physically viable pairwise transitions for acyclic leaping, Fig. 6, is constructed by hand in the same way as described in Section [1, Sec. III-C] (although the process could be automated) and specifies a formal grammar that includes six possible leaping words.

Determining which of these possible leap words are physically accessible by a particular platform through reasoning about the associated hybrid dynamics is considerably more difficult than the comparable analysis of the three-contact model in Section II-C and lies well beyond the scope of this paper. Instead, in Fig. 5 we present data arising from the two of these six logical paths that our experiments reveal—and that physical intuition (informed by the asymmetry in the appendages and the offset hip) as well as numerical simulations corroborate—should in fact represent the only leaps accessible to the Jerboa platform. The $(+,-)$ leap with RHex is more balanced than Jerboa, though slightly biased instead towards the front leg, and the robot can achieve four of the possible leap words[8] (the $(+,+)$ leap studied in [1, Sec. III-C] could reach five). However note that among these different mode sequences and associated continuous

[8]The experiments presented in [1] include some examples, for $t_2 > 0.12$, of an undesired cycle with the front legs hitting the ground a second time. This is reported here with an additional gray arrow indicating the mistaken $0001 \rightarrow 0101$ transition instead of the $0001 \rightarrow 0000$ transition that would be expected.

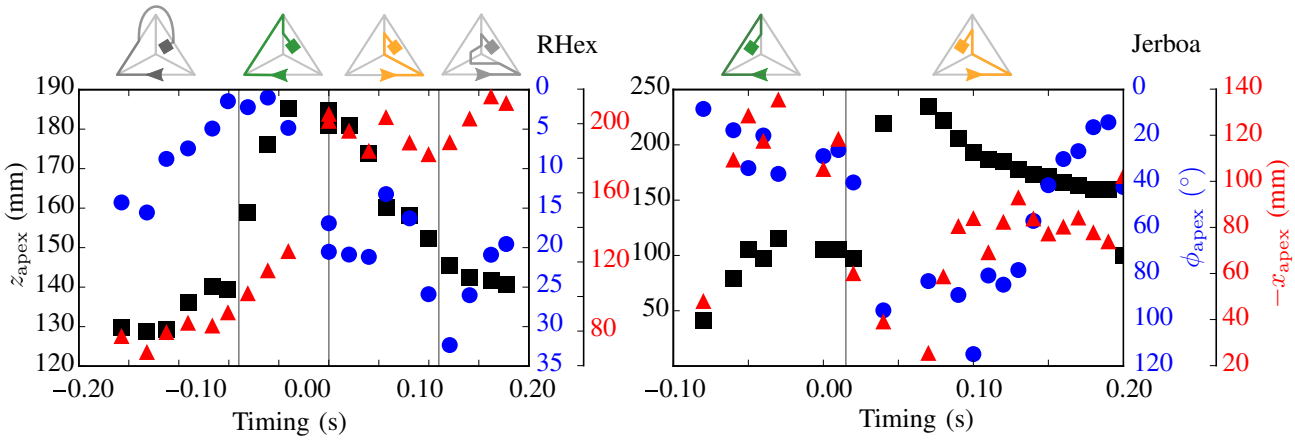

Fig. 7. Apex height relative to initial condition (black square), displacement (red triangle), and pitch (blue disk) data for $(+,-)$ leaping with Jerboa (right), compared with corresponding data from RHex [1, Fig. 5, middle] (left), generated using a Vicon motion capture system (cf. Section III).

trajectories all six possible words are represented, suggesting that for this four-contact leaping model the pairwise pruning reduced this transition graph as much as possible.

B. *Empirically found Leap Words*

We present in Fig. 7 a sweep of the family of apex states achieved by the two physically accessible Jerboa leaps juxtaposed against the closest corresponding RHex words (adapted from [1, Fig. 5]). Note that these (respectively, green and orange) traces through the GRC differ in their final "letters" according to a front/back symmetry since the Jerboa's final contact mode inevitably includes its long tail. We find it noteworthy that trends in vertical apex height (black squares) and pitch (blue circles) are roughly preserved between these different platforms (notwithstanding the different absolute measurements—Table I) as their control input timing is varied.[9] Most significantly, both machines exhibit similar discontinuities of apex state at relative timings associated with a switch between words (demarcated by the thin vertical lines in the figures). It is this significance of the word boundary discontinuity over dramatically different kinematics and mechanics that continues to motivate our study of the GRC as a potentially fundamental feature of transitional tasks in general for manipulation and self-manipulation systems, as we will remark upon more speculatively in the conclusion.

IV. Leaping Behaviors

In Table I we include some relevant parameters of the two robots examined here, RHex (specifically XRL) [4], and the tailed Jerboa [2], showing the disparate kinematic and dynamic features. We also include some metrics which we believe are the most relevant to this transitional task domain, including specific power[10], specific force[11], and specific agility[12] (maximum total energy over mass) [18] as configured for leaps presented here and in [1] (two sagittally projected appendages).

TABLE I

Specifications and Performance Metrics

	Jerboa [2]	RHex [4]
Mass m_b	2.27 kg	7.50 kg
Length, height (mm)	0.21 m × 0.10 m	0.51 m × 0.10 m
Front, rear hip offset	0.072 m (coincident)	±0.205 m
Front appendage length	0.105 m[14]	0.06–0.16 m (rolling)
Rear appendage length	0.3 m	(same as above)
Specific power[10]	376 W / kg	182 W / kg
Specific force[11] (vertical)	46 N / kg	75 N / kg
Specific agility[12] [18]	4.75 J / kg	2.24 J / kg

TABLE II

Behaviors (please see Section IV)

	Tailless Jerboa (II)	Jerboa [2] (IV)		RHex [4]	
Leg[13]	Spring	Rigid	Spring	Spring	Spring
Leaps	Single	Single	Double	Single	Double
Gap	0.27 m	0.22 m	0.42 m	0.50 m	0.60 m
	1.3 BL	1.0 BL	2.0 BL	1.0 BL	1.2 BL
Ledge	0.09 m	0.14 m	0.17 m	0.27 m	0.29 m
	0.9 HH	1.3 HH	1.6 HH	1.7 HH	1.8 HH

Our systematic exploration through the timing parameter (Fig. 7) yields a "lookup table" of sorts enabling the robot to choose among the timings the best apex condition to meet a given task. For example, to leap across a gap on Jerboa the greatest forward displacement can be attained in the $[-0.08, 0]$ s range. This method was used to attain the "single jump" statistics in Table II, where Jerboa was used with a rigid leg[13] and a tail.

[9] Unsurprisingly, we find less correspondence in horizontal displacement trends, because this projection of the apex state is the one most sensitive to friction effects.

[10] Sum over all motors of peak output power divided by robot mass.

[11] Peak vertical force with all motors at stall, accounting for effective limb length in the "sitting" condition that leaps are initiated, divided by mass.

[12] Measured empirically as the maximum apex energy obtained from the systematic trials of Section III divided by robot mass. For Jerboa, the maximum energy was 10.8 J at timing parameter +0.09 s (4.6 J vertical potential, 1.3 J forward kinetic, and 4.8 J rotational kinetic). For RHex, the maximum energy was 16.7 J at timing parameter 0 s (13.3 J vertical potential, 3.3 J horizontal kinetic, and 0.1 J rotational kinetic).

[13] The Jerboa rigid leg has a point toe while the compliant leg has rolling contact like RHex. The RHex leg was assumed effectively rigid for single jumps in [1], but limb compliance certainly plays a role in double jumps (if not single jumps as well).

To build on this baseline performance, we follow [1] in selecting an initial leap with minimal body pitch and high apex energy (looked up from Fig. 7) to prepare [23] a second step qualitatively resembling hip-energized SLIP [24] (please see [2] for more details about hip- vs tail-energized approaches to anchoring [25] variants of the SLIP template in the Jerboa body). In order to accomplish this, we introduce half-circle[14] compliant legs [26] to (i) improve the effective mechanical advantage during stance (through rolling contact), and (ii) amplify peak power output during a second step (by adding the release of stored spring energy). Half-circle legs also amplify ground reaction forces (as used to allow for greater control authority in Section II-E), however for these double jumps no torque reversal is used, since the tail actuator is available to provide additional control authority over the pitch DOF. This increased complexity of both the mechanism and controller removes these behaviors well beyond the analytical scope of this paper, however, using this "double jump" strategy, we gain drastic performance improvements as cataloged in Table II. The measurements in this table use calibrated test setups with known gap distance, ledge height, etc. Note that the monopedal ("tailless") Jerboa suffers from adverse pitch effects with a rigid leg consistent with Proposition 1 (attached video), making it incapable of ledge climbing or gap crossing without compliance.

We highlight some qualitative features of the leaps resulting from $(+,-)$ relative timing (see attached video) below:

i) **Gap crossing:** The rigid Jerboa of Section III crosses a gap slightly longer than its body with timing -0.07 s (green leap in Fig. 6), and up to two bodylengths using a double jump (half-circle compliant legs).

ii) **Ledge climbing:** Using a $+0.25$ s timing parameter, the robot hopped into a 0.14 m ledge. This is improved to 0.17 m with a double jump, raising the prospect of adding (medium-rise) stair ascent to Jerboa's behavioral repertoire.

iii) **Self-righting:** The relatively low body inertia and asymmetric appendages lead to a preponderance of leaps resulting in front-flips (as evidenced by the high apex pitch in the 0.0–0.1 s timing range in Fig. 7). This behavior has applications in rapid, dynamic self-righting.

Lastly, note that since the experiments presented in this section don't depend on any sensory feedback (except reliable encoder signals), the trials are repeatable with identical initial conditions. A full statistical analysis is deferred to future work.

V. Conclusions and Further Work

In this paper, we further the work started in [1] of introducing guiding principles to the challenging study of transitional hybrid dynamical behaviors such as legged leaping. To our knowledge, the pairing of a formal hybrid system framework, [5], with the discrete leaping "grammar", [1], that led to our main analytical result (Prop. 1)—while specific in scope—is the first of its kind in the literature. In addition to this conceptual contribution, we develop, using a combination of analytical (Section II), numerical (Section III), and intuitive reasoning, leaping behaviors for the Penn Jerboa that allow it to match or exceed RHex in performance (Section IV). In the process, we empirically verify an aspect of "robustness" in the GRC over different platforms (Fig. 7), and leverage it as a tool not only for analyzing, but also developing leaping behaviors.

Even though the platforms that have so far benefited from the GRC for organizing leaping behaviors (RHex [1] and Jerboa, to our knowledge) have some morphological similarities (revolute singly-actuated legs, usable body contacts), their disparity in contact specifics (tail is a sliding contact), kinematics and dynamics (Table I) suggests that this research is applicable to a broad class of multi-appendage robots, where making or breaking contact with the ground induces a significant change in the dynamics.

While Fig. 7 is visually appealing, and suggests some underlying common structural relation between the hybrid dynamical executions on the two platforms, we presently have no means of quantitatively verifying, much less explaining, this phenomenon. The two machines' similarly abrupt apex state transitions relative to leap word boundaries (the thin vertical lines of Fig. III-A), suggests a correspondence between the topological significance of the symbolic boundary in the combinatorial space (chains over the GRC poset) and that of its realization in the continuous space of trajectories. This prospect strongly motivates our study of the GRC as potentially representing a fundamental feature of transitional tasks in general for manipulation and self-manipulation systems.

The fledgling analytical steps we have taken in this paper (Prop. 1) suggest a "proof technique" that has a large potential of application to previously (analytically) intractable hybrid transitional behaviors. In the near term, an analysis of leaps in the 4-contact GRC is warranted, and would open up the possibility of even greater leaping performance being extracted from such power- and force-limited machines.

[14]The rest-diameter of the half-circle leg is the same as the length of the rigid leg, as in Table I.

References

[1] A. M. Johnson and D. E. Koditschek, "Toward a vocabulary of legged leaping," in *Proc. IEEE Intl. Conf. Robotics and Automation*, May 2013, pp. 2553–2560.

[2] A. De and D. E. Koditschek, "The Penn Jerboa: A platform for exploring parallel composition of templates," University of Pennsylvania, Tech. Rep., February 2015, arXiv:1502.05347 [cs.RO]. [Online]. Available: http://repository.upenn.edu/ese_reports/16

[3] M. Raibert, *Legged Robots that Balance*, ser. Artificial Intelligence. MIT Press, 1986.

[4] G. C. Haynes, J. Pusey, R. Knopf, *et al.*, "Laboratory on legs: an architecture for adjustable morphology with legged robots," in *Unmanned Systems Technology XIV*, vol. 8387, no. 1. SPIE, 2012.

[5] A. M. Johnson, S. E. Burden, and D. E. Koditschek, "A hybrid systems model for simple manipulation and self-manipulation systems," *arXiv Preprint*, 2015, arXiv:1502.01538 [cs.RO]. [Online]. Available: http://arxiv.org/abs/1502.01538

[6] A. M. Johnson and D. E. Koditschek, "Legged self-manipulation," *IEEE Access*, vol. 1, pp. 310–334, May 2013.

[7] R. M. Alexander, "Three uses for springs in legged locomotion," *The Int. J. Robotics Research*, vol. 9, no. 2, pp. 53–61, 1990.

[8] T. Libby, T. Y. Moore, E. Chang-Siu, *et al.*, "Tail-assisted pitch control in lizards, robots and dinosaurs," *Nature*, vol. 481, no. 7380, pp. 181–184, January 2012.

[9] A. O. Pullin, N. Kohut, D. Zarrouk, and R. Fearing, "Dynamic turning of 13 cm robot comparing tail and differential drive," in *Proc. IEEE Intl. Conf. Robotics and Automation*, May 2012, pp. 5086–5093.

[10] R. Briggs, J. Lee, M. Haberland, and S. Kim, "Tails in biomimetic design: Analysis, simulation, and experiment," in *Intelligent Robots and Systems, IEEE/RSJ Int. Conf.*, 2012, pp. 1473–1480.

[11] G.-H. Liu, H.-Y. Lin, H.-Y. Lin, *et al.*, "A Bio-Inspired Hopping Kangaroo Robot with an Active Tail," *J. Bionic Engineering*, vol. 11, no. 4, pp. 541–555, 2014.

[12] A. De and D. E. Koditschek, "Parallel composition of templates for tail-energized planar hopping," in *Proc. IEEE Intl. Conf. Robotics and Automation*, 2015, pp. 4562–4569.

[13] G. J. Zeglin, "Uniroo–a one legged dynamic hopping robot," B.S. Thesis, Massachusetts Institute of Technology, 1991.

[14] A. Patel and M. Braae, "Rapid acceleration and braking: Inspirations from the cheetah's tail," in *Proc. IEEE Intl. Conf. Robotics and Automation*, 2014, pp. 793–799.

[15] K. Autumn, M. Buehler, M. Cutkosky, *et al.*, "Robotics in scansorial environments," in *Defense and Security*. SPIE, 2005, pp. 291–302.

[16] A. Crespi, K. Karakasiliotis, A. Guignard, and A. J. Ijspeert, "Salamandra robotica ii: an amphibious robot to study salamander-like swimming and walking gaits," *IEEE Trans. Robotics*, vol. 29, no. 2, pp. 308–320, 2013.

[17] S. M. O'Connor, T. J. Dawson, R. Kram, and J. M. Donelan, "The kangaroo's tail propels and powers pentapedal locomotion," *Biology Letters*, vol. 10, no. 7, July 2014.

[18] J. M. Duperret, G. D. Kenneally, J. L. Pusey, and D. E. Koditschek, "Towards a comparative measure of legged agility," in *Int. Symp. on Experimental Robotics*, June 2014.

[19] P. Holmes, R. J. Full, D. E. Koditschek, and J. Guckenheimer, "The dynamics of legged locomotion: Models, analyses, and challenges," *SIAM Review*, vol. 48, no. 2, pp. 207–304, 2006.

[20] H. Edelsbrunner and J. Harer, *Computational Topology: An Introduction*. Providence, RI: American Mathematical Soc., 2010.

[21] D. McMordie and M. Buehler, "Towards pronking with a hexapod robot," in *Int. Conf. Climbing and Walking Robots*, Karlsruhe, Germany, September 2001.

[22] A. De, G. Lynch, A. Johnson, and D. Koditschek, "Motor sizing for legged robots using dynamic task specification," in *Proc. IEEE Intl. Conf. Technologies for Practical Robot Applications*, April 2011, pp. 64–69.

[23] R. Burridge, A. Rizzi, and D. Koditschek, "Sequential composition of dynamically dexterous robot behaviors," *The Int. J. Robotics Research*, vol. 18, pp. 534–555, 1999.

[24] Z. H. Shen and J. E. Seipel, "A fundamental mechanism of legged locomotion with hip torque and leg damping," *Bioinspiration & Biomimetics*, vol. 7, no. 4, p. 046010, 2012.

[25] R. Full and D. Koditschek, "Templates and anchors: Neuromechanical hypotheses of legged locomotion on land," *J. of Experimental Biology*, vol. 202, no. 23, pp. 3325–3332, 1999.

[26] E. Z. Moore, D. Campbell, F. Grimminger, and M. Buehler, "Reliable stair climbing in the simple hexapod RHex," in *Proc. IEEE Intl. Conf. Robotics and Automation*, vol. 3, 2002, pp. 2222–2227.